Repeatability, interocular correlation and agreement of optic nerve head vessel density in healthy eyes: a swept-source optical coherence tomographic angiography study

Dan−Qi Fang[1], Da−Wei Yang[2], Xiao−Ting Mai[1], Carol Y Cheung[2], Hao−Yu Chen[1]

[1]Joint Shantou International Eye Center, Shantou University & the Chinese University of Hong Kong, Shantou 515041, Guangdong Province, China

[2]Department of Ophthalmology and Visual Sciences, Chinese University of Hong Kong, Hong Kong 999077, China

Correspondence to: Hao-Yu Chen. Joint Shantou International Eye Center, North Dongxia Road, Shantou 515041, Guangdong Province, China. drchenhaoyu@gmail.com

Abstract

● **AIM:** To assess the repeatability, interocular correlation, and agreement of quantitative swept-source optical coherence tomography angiography (OCTA) optic nerve head (ONH) parameters in healthy subjects.

● **METHODS:** Thirty-three healthy subjects were enrolled. The ONH of both eyes were imaged four times by a swept-source-OCTA using a 3 mm ×3 mm scanning protocol. Images of the radial peripapillary capillary were analyzed by a customized Matlab program, and the vessel density, fractal dimension, and vessel diameter index were measured. The repeatability of the four scans was determined by the intraclass correlation coefficient (ICC). The most well-centered optic disc from the four repeated scans was then selected for the interocular correlation and agreement analysis using the Pearson correlation coefficient, ICC and Bland-Altman plots.

● **RESULTS:** All swept-source-OCTA ONH parameters exhibited certain repeatability, with ICC>0.760 and coefficient of variation (CoV)≤7.301%. The obvious interocular correlation was observed for papillary vessel density (ICC=0.857), vessel diameter index (ICC=0.857) and fractal dimension (ICC=0.906), while circumpapillary vessel density exhibited moderate interocular correlation (ICC=0.687). Bland-Altman plots revealed an agreement range of -5.26% to 6.21% for circumpapillary vessel density.

● **CONCLUSION:** OCTA ONH parameters demonstrate good repeatability in healthy subjects. The interocular correlations of papillary vessel density, fractal dimension and vessel diameter index are high, but the correlation for circumpapillary vessel density is moderate.

● **KEYWORDS:** interocular correlation; repeatability; optic nerve head; optical coherence tomography angiography; vessel density

INTRODUCTION

The optic nerve head (ONH) is a crucial structure in the central nervous system, as it is the only part that can be observed directly during the clinical examination. The evaluation of the ONH and its surrounding tissues provides essential information for diagnosing and assessing various ocular and neurological diseases, including glaucoma[1-2], optic neuritis[3-5], and Alzheimer's disease[6]. Initially, ophthalmoscopy was used to assess the color, cup-disc ratio, and neuroretinal rim loss of the ONH[7]. The introduction of optical coherence tomography (OCT) made it possible to quantitatively measure the thickness of the peripapillary retinal nerve fiber layer[8]. More recently, optical coherence tomography angiography (OCTA) has been applied to the examination of the ONH. OCTA is a non-invasive, dye-free, and fast method that provides three-dimensional imaging of capillary plexuses. It has been shown that the health of the ONH is closely related to its microvascular circulation[9-10]. Several studies have investigated the ONH and peripapillary vessel density measured by OCTA in both healthy and diseased subjects, including those with glaucoma[11-13], diabetic retinopathy[14-15], dysthyroid optic neuropathy[16], and Behcet's disease[17]. These studies have provided valuable insights into the relationship between ONH metrics and various ocular and neurological conditions.

The human body exhibits bilateral mirror-symmetry with paired eyes, ears, and limbs. A median sagittal plane divides the human body into two highly similar halves. It has been known that various binocular metrics show more similar characteristics than those obtained from unrelated individuals[18]. Understanding interocular symmetry or asymmetry is valuable in scientific research and clinical practice. In scientific research, the principle of symmetry often permits the study of just one eye, using the fellow eye as a "control"[19]. In clinical practice, previous studies have suggested that excessive interocular asymmetry in intraocular pressure, retinal nerve fibre layer and appearance of the optic disc are important in diagnosing glaucoma[20-22]. Our prior study showed an excellent interocular correlation in the foveal avascular zone area, but poor interocular correlation in macular vessel density[23].

The current study aims to investigate the interocular correlation and agreement of ONH vessel density in healthy subjects.

SUBJECTS AND METHODS

Ethical Approval The study adhered to the principles of the Declaration of Helsinki, and was approved by the Institutional Review Board of Joint Shantou International Eye Center of Shantou University and the Chinese University of Hong Kong, approval number: 19-004. After an explanation of the nature of the study, written informed consent approved by the institutional review board was obtained from all participants.

Study Subjects This cross-sectional observational study enrolled healthy Chinese subjects aged between 18 and 40y. All participants underwent four consecutive OCTA examinations of both eyes using OCTA devices operated by a single technician in the same environment. Inclusion criteria required subjects to have a best-corrected visual acuity of 6/6 or better using the Snellen chart, intraocular pressure less than 21 mm Hg, refractive error within ±6 D, no evidence of systemic or ocular diseases and adequate pupillary dilation. Low image quality scans were excluded, defined as scans with a quality index less than 60. The participants with abnormal findings on OCTA exams or complaints of visual symptoms were also excluded.

To ensure adequate statistical power, sample size calculations were performed for both repeatability and agreement. For repeatability, the formula,

$$1.96 \times \frac{S_w}{\sqrt{2n(m-1)}} = 15\% \times S_w$$

was used, where S_w represents the within-subject standard deviation, and the 95% confidence interval (CI) of S_w was set at 15% either side of the estimate of S_w. The simplified formula $n=1.96/[2(m-1)\times 0.15]$ (where n is the sample size, and m is the number of observation times) was used to calculate the required sample size[24]. In this study, four measurements

on each of the 33 subjects were required. For agreement, the sample size calculation was based on the formula

$$n \geq \frac{\log(1-\beta)}{\log(1-\alpha)}$$

where n represents the sample size, α is the discordance rate, and β is the tolerance probability[25]. When $\alpha=0.05$ and $\beta=80\%$, $n \geq 32$. Based on these calculations, we determined that a total of 33 subjects would provide adequate statistical power for this study, with four measurements per subject.

Optical Coherence Tomography Angiography Imaging
This study employed a swept-source OCTA device (Topcon DRI OCT Triton) to acquire OCTA images, using ONH 3 mm×3 mm mode with a resolution of 320×320 A-scans protocol. The DRI-OCT Triton utilizes a tunable wavelength ranging from 1000 to 1100 nm, a scan rate of 100 kHz and a depth resolution of 8 μm. During the angiographic process, the DRI-OCT uses the proprietary OCTA algorithm OCTARA™ for OCTA ratio analysis of motion contrast[26-27]. Based on the automated layer segmentation algorithm, the built-in ophthalmic data management platform, IMAGEnet6, generates an en-face image of the superficial radial peripapillary capillary map from the surface to 130 μm below the internal limiting membrane, which predominantly comprises capillary beds within retinal nerve fiber layer.

Both eyes of each subject were scanned four times continuously. The pupils were dilated with one or two drops of topical 0.5% tropicamide, ensuring a diameter of at least 6 mm. Participants were instructed to close their eyes between sequential scans. The eye-tracking function was used and the images were assessed immediately after each scan. The scans with low image quality were eliminated, and additional scans were performed. The OCTA image with poor quality was defined as having a quality score below 60, motion artefacts (*e.g.*, discontinuing or doubling of the retinal vessels), or inaccurate segmentation of retinal layers.

Quantitative Assessment of Nerve Head Capillary Network
The nerve head capillary OCTA images were quantified using a customized Matlab program (MATLAB R2017a, MathWorks, Natick, MA, USA), which has been thoroughly described in our previous publications[28-30]. The automation of the analysis process ensures objectivity and minimizes the potential for observer bias. Additionally, the use of a masked investigator further increases the reliability and accuracy of the results.

In this study, several metrics were used to analyze the OCTA images. The papillary region is defined as a circle whose boundary is fitted to the optic disc, and the circumpapillary region is between the outline of the disc and the circle with a diameter of 3 mm. The circumpapillary region is radially divided into eight 45° sections. The two 45° sections in the temporal part were combined and defined as the temporal

Table 1 The means, standard deviation and intrasession repeatability of optic nerve head metrics for right and left eyes

Parameters	Right eye					Left eye				
	Mean±SD	S_w	CoV	Precision	ICC	Mean±SD	S_w	CoV	Precision	ICC
Temporal vessel density (%)	65.56±6.90	3.541	5.402	6.941	0.920	71.03±5.84	2.991	4.211	5.863	0.921
Temporal superior vessel density (%)	70.53±4.57	2.693	3.819	5.278	0.886	74.05±4.57	2.624	3.544	5.144	0.895
Temporal inferior vessel density (%)	71.18±4.67	2.873	4.036	5.630	0.871	73.01±5.43	3.172	4.344	6.217	0.889
Nasal superior vessel density (%)	69.50±5.26	2.586	3.721	5.069	0.928	66.76±5.10	3.838	5.749	7.523	0.760
Nasal inferior vessel density (%)	66.97±5.53	3.001	4.481	5.881	0.908	66.13±5.03	3.099	4.686	6.073	0.871
Nasal vessel density (%)	60.01±6.87	2.679	4.464	5.250	0.958	55.48±6.54	3.622	6.528	7.099	0.903
Circumpapillary vessel density (%)	67.29±3.08	1.828	2.717	3.583	0.884	67.74±3.14	2.089	3.083	4.094	0.839
Papillary vessel density (%)	54.52±4.19	1.816	3.330	3.559	0.947	54.06±4.57	1.919	3.551	3.762	0.951
Vessel diameter index (mm)	0.016±0.002	0.001	5.475	0.002	0.922	0.016±0.002	0.001	7.301	0.002	0.875
Fractal dimension	1.561±0.023	0.008	0.525	0.016	0.967	1.560±0.025	0.010	0.643	0.020	0.955

SD: Standard deviation; CoV: Coefficient of variation; ICC: Intraclass correlation coefficient; OCTA: Optical coherence tomography angiography; S_w: Within-subject standard deviation.

region. And the two 45° sections in the nasal part were combined and defined as the nasal region. The remaining regions are defined as temporal superior, temporal inferior, nasal superior and nasal inferior regions (Figure 1). Vessel density was calculated as the ratio of the area occupied by white pixels (*i.e.*, blood vessel) to the total area in the target region. Fractal dimension was then calculated using the box-counting method, which is a widely accepted technique to quantify the complexity and irregularity of a structure. In the context of retinal vasculature, fractal dimension can be considered as an indicator of vascular tortuosity or the degree of branching and looping in the blood vessels. Vessel diameter index (VDI) was the average vessel caliber in the OCTA image.

The interocular correlation and agreement analysis was performed using the images of the optic disc with the most centered position from the four repeated scans in each eye. The selected images were then used to compare the vasculature structure and metrics between the two eyes.

Statistical Analysis All the quantitative data were summarized as mean±standard deviation (SD). Statistical analysis was processed using SPSS (version 21.0; SPSS, Inc., Chicago, IL, USA). A *P*-value less than 0.05 was deemed statistically significant in all analyses.

The following parameters were calculated to assess the repeatability of four repeated measurements: within-subject standard deviation (S_w), precision (repeatability coefficient; $1.96 \times S_w$), coefficient of variation (CoV) ($100 \times S_w$/overall mean) and intraclass correlation coefficient (ICC).

Paired *t*-test was used to determine the significance of interocular differences. Pearson's correlation and ICC were performed to assess the correlation between the two eyes. ICC values greater than or equal to 0.9 are classified as excellent, good for those between 0.75 and 0.9, moderate for those between 0.5 and 0.75, and poor if less than 0.5. The Bland-
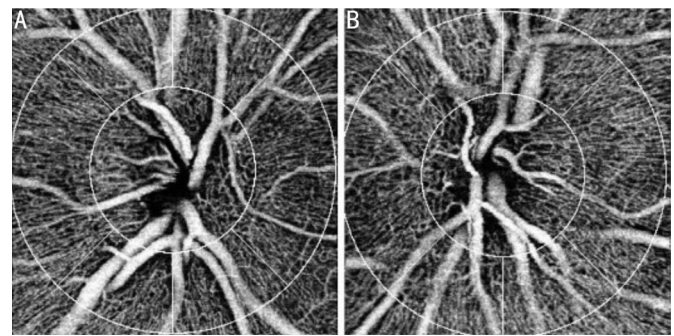

Figure 1 Optical coherence tomography angiography image of optic disc scans in right (A) and left eyes (B) from a normal subject Vessel density measurements were made in the eight subfields: central (papillary), temporal, temporal superior, temporal inferior, nasal, nasal superior, nasal inferior, and circumpapillary regions.

Altman plots were generated to show the agreement between the two eyes, by calculating the difference between them and plotting it against the mean value. Horizontal dashed lines were drawn at the 95% limits of agreement (95%LoA), defined as the mean difference ±1.96×SD of the differences.

RESULTS

In this study, 66 eyes of 33 healthy volunteers (10 men and 22 women) were enrolled. The mean age of the participants was 24.9±2.5y (ranged from 20 to 35y). The mean spherical equivalent of refractive error (SE) was -2.33±1.93 D (ranged from -5.50 to +0.75 D) in the right eye and -2.27±2.11 D (ranged from -5.75 to +0.75 D) in the left eye. The mean image quality index was 69.8±3.30 (ranged from 60 to 72) in the right eye and 71.1±2.57 (ranged from 64 to 75) in the left eye. There was no statistical significance in refractive error (*P*=0.666) between the two eyes.

Table 1 shows the mean, standard deviation and repeatability of ONH metrics for the right and left eyes. All the metrics demonstrated good to excellent repeatability, with ICC value greater than 0.760 and CoV values less than or equal to

Table 2 Correlation coefficients of the OCTA optic nerve head vessel metrics between the two eyes

Parameters	Paired *t*-test *P*	Intraclass correlation	Pearson correlation	Pearson correlation *P*
Temporal vessel density	<0.001	0.649	0.649	<0.001
Temporal superior vessel density	<0.001	0.368	0.354	0.043
Temporal inferior vessel density	0.192	0.620	0.455	0.008
Nasal superior vessel density	0.087	0.523	0.378	0.030
Nasal inferior vessel density	0.347	0.578	0.419	0.015
Nasal vessel density	<0.001	0.626	0.632	<0.001
Circumpapillary vessel density	0.357	0.687	0.522	0.002
Papillary vessel density	0.529	0.857	0.746	<0.001
Vessel diameter index	0.171	0.857	0.758	<0.001
Fractal dimension	0.668	0.906	0.825	<0.001

OCTA: Optical coherence tomography angiography.

Table 3 Summary of the interocular agreement of the OCTA optic nerve head vessel metrics between the two eyes

Parameters	Mean absolute difference	Mean difference	95%CI	Range of agreement
Temporal vessel density (%)	6.05±3.60	5.04±4.96	-4.68, 14.76	19.43
Temporal superior vessel density (%)	5.36±4.18	4.71±4.93	-4.94, 14.36	19.31
Temporal inferior vessel density (%)	4.80±3.35	1.34±5.76	-9.94, 12.62	22.56
Nasal superior vessel density (%)	4.10±3.08	-1.52±4.94	-11.21, 8.17	19.38
Nasal inferior vessel density (%)	4.76±3.50	-0.98±5.88	-12.50, 10.55	23.06
Nasal vessel density (%)	6.63±4.42	-5.74±5.56	-16.63, 5.16	21.79
Circumpapillary vessel density (%)	2.42±1.67	0.48±2.93	-5.26, 6.21	11.47
Papillary vessel density (%)	2.44±1.97	-0.35±3.15	-6.52, 5.82	12.34
Vessel diameter index (mm)	0.0010±0.0008	0.0003±0.0012	-0.0021, 0.0027	0.0048
Fractal dimension	0.0113±0.0070	-0.0010±0.0134	-0.0273, 0.0252	0.0525

OCTA: Optical coherence tomography angiography; CI: Confidence interval.

7.301%. The temporal vessel density was found to be higher than the nasal part in both eyes.

The paired *t*-test, Pearson correlation and ICC between the two eyes are presented in Table 2. Generally, there was no significant difference (*P*>0.05) between the two eyes in papillary and circumpapillary vessel density, fractal dimension or VDI except for the vessel density in some sectors. Papillary vessel density (ICC=0.857, *r*=0.746), VDI (ICC=0.857, *r*=0.758) and fractal dimension (ICC=0.906, *r*=0.825) showed good to excellent correlation between the two eyes. The correlation of circumpapillary vessel density (ICC=0.687, *r*=0.522) showed moderate interocular correlation, except in the temporal superior sector. The scatter plots and correlation analysis are also presented in Figures 2 and 3.

Table 3 and Figures 2-3 demonstrate the agreement of the OCTA ONH vessel metrics between the two eyes. The 95%LoA was from -6.52% to 5.82% for papillary vessel density and from -5.26% to 6.21% for circumpapillary vessel density.

DISCUSSION

This study was conducted to assess the intraocular repeatability and interocular symmetry of ONH OCTA metrics in healthy subjects. The results showed that papillary vessel density

(ICC=0.857), VDI (ICC=0.857) and fractal dimension (ICC=0.906) demonstrated good or excellent correlation between the two eyes. Circumpapillary vessel density, with the exception of the temporal superior sector, showed moderate interocular correlation (ICC=0.687). Bland-Altman plots revealed the normal range of agreement for ONH metrics. This information can offer statistical advice to authors who are conducting OCTA research. It assists them in selecting suitable data from either one eye or both eyes. Additionally, in clinical practice, this information can be valuable in determining whether the difference between two eyes is within the normal range.

Measurements obtained from both the right and left eyes generally exhibit a correlation[31]. In scientific research, it is crucial to carefully consider how data from one or both eyes are collected and analyzed. In the one-eye studies, various criteria were employed for selection, including the right eye, left eye, a randomly chosen eye, or the dominant eye. In two-eye studies, some researchers utilized data from one eye and used the fellow eye as a control, while others used data from unrelated subjects. Additionally, some employed data from both eyes but analyzed them separately, while others combined data from both eyes[32]. However, a significant proportion of
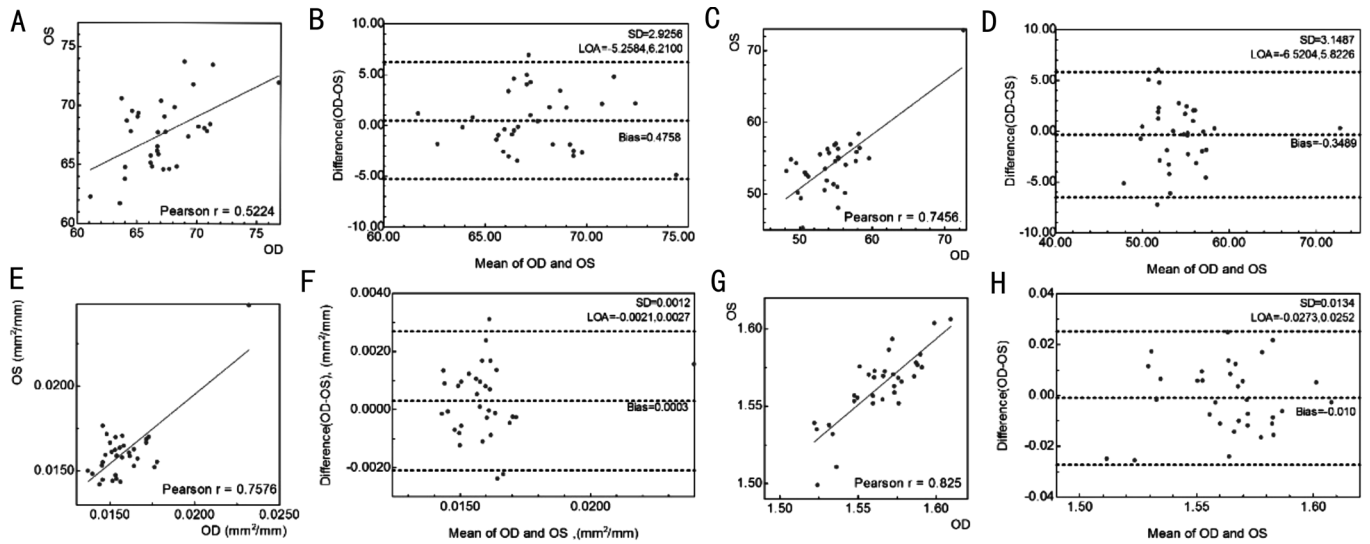
Figure 2 Scatter plots (A, C, E, G) and Bland-Altman plots (B, D, F, H) of the circumpapillary vessel density (A, B), papillary vessel density (C, D), vessel diameter index (E, F) and fractal dimension (G, H) of the two eyes measured by Triton optical coherence tomography angiography.
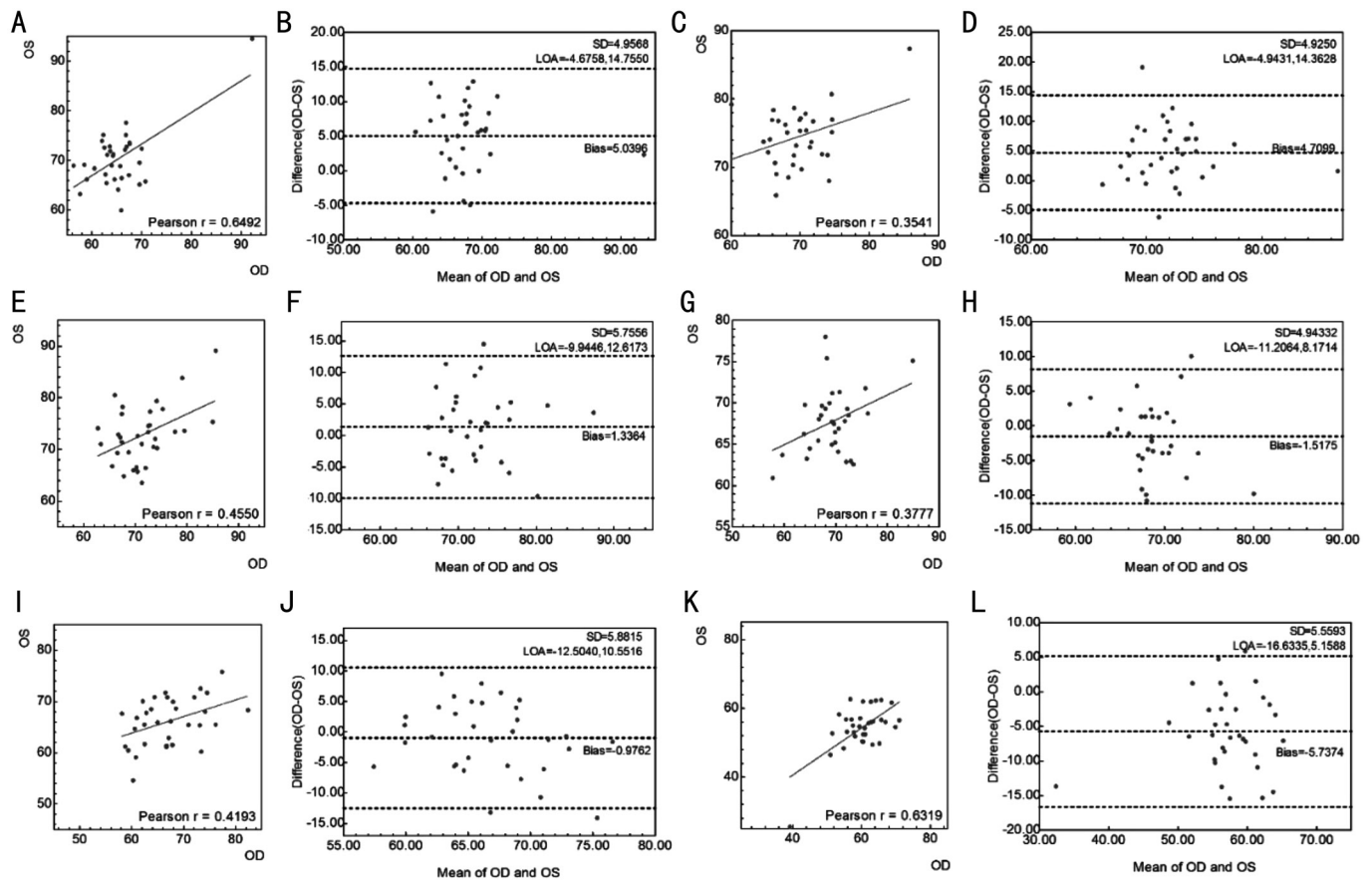

Figure 3 Scatter plots and Bland-Altman plots of different sectors of circumpapillary vessel density of the two eyes measured by Triton optical coherence tomography angiography A, B: Temporal sector; C, D: Temporal superior sector; E, F: Temporal inferior sector; G, H: Nasal superior sector; I, J: Nasal inferior sector; K, L: Nasal sector. OD: *Oculus dextrus*; OS: *Oculus sinister*.

studies did not describe the basic for selection criteria clearly or used inappropriate statistical methods[31]. When the two eyes data are combined in the same group, the ignorance of interocular correlation between the eyes of the same subject can lead to inaccurate estimates of standard errors of coefficients and *P*-values. What's more, it is important to note

that using the fellow eye of the same subject as a control can be a better choice than using an eye from a different subject when the metrics of both eyes show good intraclass correlation and a narrow range of agreement[33]. Proper statistical analysis is essential to draw valid conclusions in such studies, ignoring interocular correlation can lead to misleading results.

The comparison and correlation of ONH vascular density between the two eyes have been previously reported in the literature. Fernández-Vigo et al[34] using Triton found no significant differences in vessel density between the fellow eyes of 33 subjects ($P\geq0.139$), although the Pearson coefficients were low (ranging from -0.242 to 0.084 in different quadrants). The current study found that the Pearson correlation coefficients between the two eyes ranged from 0.378 to 0.649 in different sectors, and the circumpapillary vessel density was 0.522. In addition to the Pearson correlation, this study further investigated the ICC. The advantage of ICC is that it provides information on the similarity, not just the correlation between the two eyes. Papillary vessel density (ICC=0.857) demonstrated a good or excellent correlation between eyes. Circumpapillary vessel density showed moderate interocular correlation (ICC=0.687), except for the temporal superior sector. These findings suggest that the contralateral eye is a suitable choice as a control compared to the eyes of unrelated subjects.

For paired organs, the measurements of the fellow organs have been shown to be significant factors in diagnosing the selected organ[35]. The evaluation of ONH metrics is valuable in assessment of various conditions, especially glaucoma[36]. Strength of interocular asymmetry can offer valuable insights for glaucoma diagnosis. The study by Hou et al[37] investigated the inter-eye ONH vessel density asymmetry, which is defined as the absolute difference between two eyes, in healthy subjects, glaucoma suspects and glaucoma patients. The inter-eye peripapillary vessel density asymmetry was found to be 1.7% (95%CI 0.8%-2.6%) in healthy subjects, 2.0% (95%CI 1.3%-4.1%) in suspect and 2.2% (95%CI 1.3%-4.3%) in glaucoma. The area under the curve of inter-eye asymmetry was 0.63 for both glaucoma suspects and glaucoma patients. In the study by Xu et al[38], the absolute difference in peripapillary vessel density between the two eyes was 2.16%±1.74% in healthy subjects, increased to 4.54%±3.46% in early to moderate primary open-angle glaucoma, and 6.35%±5.18% in total primary open-angle glaucoma. Both studies used the Optovue device, while this study used the Triton device. The Triton device, utilizing FastTrac technology, efficiently tracks eye movements and rescans only areas impacted by motion artifacts to minimize motion errors[39]. Optovue also integrates an eye-tracking system in its OCTA imaging and has introduced a software-based method in which OCTA volumes of the same retinal area are acquired repeatedly with horizontal and then vertical scans[40]. A previous study shows that the Triton device demonstrated superior performance compared to Optovue in terms of image artifacts, with statistically significant differences observed in the superficial capillary layer[39]. Triton's superior performance is likely due to its use

of SS-OCT technology at a 1050 nm wavelength. The longer wavelength is less susceptible to light scattering, thereby enhancing image quality.

In this study, the absolute difference in circumpapillary vessel density was 2.42%±1.67%, which is comparable to the study of Xu et al[38] and higher than the study of Hou et al[37]. Unlike previous studies, this study analyzed not only the mean absolute difference but also the 95%LoA. The mean and standard deviation of absolute difference would suggest that the difference greater than the higher limit of asymmetry is abnormal, which is not correct. The mean difference and 95%LoA avoid this issue. This study suggests that an interocular difference greater than 6.21% in circumpapillary vessel density should be considered abnormal. Figure 3B, 3D, 3F, show significant data dispersion, with many subjects along the mark of 10 units difference in vessel density. The interocular agreement is better for the total circumpapillary vessel density than for vessel density in specific sectors (Table 3). This discrepancy may result from the distribution of retinal vessels, which is not symmetric between the two eyes.

As far as current understanding extends, no studies have investigated the symmetry of ONH VDI and fractal dimension. VDI is a parameter that represents the average vessel caliber in the OCTA image. It was reported that larger peripapillary vessels showed an increased vessel dimension index in non-proliferative diabetic retinopathy eyes[41]. This study showed a good intraclass correlation (ICC=0.857) between the two eyes. This result suggests that the fellow eye can be used as a control. The agreement analysis suggests that an interocular difference of VDI greater than 0.0027 mm can be considered abnormal.

Fractal dimension is a parameter for the complexity of vascular morphology. A previous study found that decreased circumpapillary fractal dimension was associated with decreased retinal nerve fibre layer thickness in primary angle-closure glaucoma and normal-tension glaucoma eyes[30]. Another study reported no statistically significant difference in fractal dimension between the two eyes on optic disc-centered fundus photography in normal subjects[42]. This study further shows an excellent ICC of fractal dimension between the two eyes, so the fellow eye should be used as a control. The agreement analysis suggests that an interocular difference greater than 0.0252 should be considered abnormal.

The repeatability of OCTA ONH metrics in Triton has been reported in the literature. Akil et al's[43] study also demonstrates excellent repeatability of the optic disc region 3 mm×3 mm scan in Triton (ICC>0.9). However, they only analyzed the full-thickness vessel density, not the superficial vessel density. Lei et al[44] reported that the ICC for the repeatability of superficial peri-papillary capillary in Triton is 0.84. Fernández-

Vigo *et al*'s[45] study found that the reproducibility coefficients of superficial vessel density measurements were higher in the central ONH (ICC=0.941) compared to peripapillary subfields (ICC: 0.499–0.853) in Triton's 6 mm×6 mm scan. This study reveals that Triton exhibits excellent or good repeatability across all subfields (ICC>0.760 and CoV≤7.301%).

There are some limitations in the current study. First, because of the shadow artifacts on the deeper layer, only the superficial capillary plexus was selected for analysis. Second, there may be out-of-range artifacts. When the center of the ONH is not at the center of the image, there may be a circumpapillary region out of the range of the scan. This may underestimate the intraocular correlation and overestimate the range of interocular agreement. Third, this study only investigated healthy subjects, and further studies with patients should be conducted.

In conclusion, quantitative OCTA ONH metrics by Triton show good repeatability in healthy subjects. There is a high inter-eye correlation in papillary vessel density, fractal dimension and VDI, moderate correlation in circumpapillary vessel density in healthy subjects. This information would be valuable for choosing proper controls in scientific research and interpreting whether the difference between two eyes is within the normal range.

ACKNOWLEDGEMENTS

REFERENCES

1 Wang YX, Panda-Jonas S, Jonas JB. Optic nerve head anatomy in myopia and glaucoma, including parapapillary zones alpha, beta, gamma and delta: Histology and clinical features. *Prog Retin Eye Res* 2021;83:100933.

2 Tao YL, Tao LM, Jiang ZX, Liu HT, Liang K, Li MH, Zhu XS, Ren YL, Cui BJ. Parameters of ocular fundus on spectral-domain optical coherence tomography for glaucoma diagnosis. *Int J Ophthalmol* 2017;10(6):982-991.

3 Petzold A, Fraser CL, Abegg M, *et al*. Diagnosis and classification of optic neuritis. *Lancet Neurol* 2022;21(12):1120-1134.

4 MacIntosh PW, Kumar SV, Saravanan VR, Shah VM. Acute changes in ganglion cell layer thickness in ischemic optic neuropathy compared to optic neuritis using optical coherence tomography. *Int J Ophthalmol* 2020;13(1):120-123.

5 Shi W, Zhang HT, Zuo HX, Li SY, Zheng PP, Xu QG, Cai SY, Wei SH, Li L, Peng CX. Structural-visual functional relationships detected by optical coherence tomography in varying age-cohorts' patients with optic neuritis. *Int J Ophthalmol* 2022;15(6):967-974.

6 Lemmens S, van Craenendonck T, van Eijgen J, De Groef L, Bruffaerts R, de Jesus DA, Charle W, Jayapala M, Sunaric-Mégevand G, Standaert A, Theunis J, van Keer K, Vandenbulcke M, Moons L, Vandenberghe R, De Boever P, Stalmans I. Combination of snapshot hyperspectral retinal imaging and optical coherence tomography to identify Alzheimer's disease patients. *Alzheimers Res Ther* 2020;12(1):144.

7 Liu Y, Wu F, Lu L, Lin D, Zhang K. Videos in clinical medicine. Examination of the retina. *N Engl J Med* 2015;373(8):e9.

8 Lin A, Mai X, Lin T, Jiang Z, Wang Z, Chen L, Chen H. Research trends and hotspots of retinal optical coherence tomography: a 31-year bibliometric analysis. *J Clin Med* 2022;11(19):5604.

9 Pujari A, Bhaskaran K, Sharma P, Singh P, Phuljhele S, Saxena R, Azad SV. Optical coherence tomography angiography in neuro-ophthalmology: Current clinical role and future perspectives. *Surv Ophthalmol* 2021;66(3):471-481.

10 Nishida T, Moghimi S, Wu JH, Chang AC, Diniz-Filho A, Kamalipour A, Zangwill LM, Weinreb RN. Association of initial optical coherence tomography angiography vessel density loss with faster visual field loss in glaucoma. *JAMA Ophthalmol* 2022;140(4):319-326.

11 Rao HL, Pradhan ZS, Suh MH, Moghimi S, Mansouri K, Weinreb RN. Optical coherence tomography angiography in glaucoma. *J Glaucoma* 2020;29(4):312-321.

12 Li YJ, Liu WS, Bai ZC, Cao RX, Ren HH. Diagnostic performance of OCT and OCTA in less than 60-year-old patients with early POAG: a cross-sectional study. *Int J Ophthalmol* 2020;13(12):1915-1921.

13 Köse HC, Tekeli O. Optical coherence tomography angiography of the peripapillary region and macula in normal, primary open angle glaucoma, pseudoexfoliation glaucoma and ocular hypertension eyes. *Int J Ophthalmol* 2020;13(5):744-754.

14 Cao D, Yang D, Yu H, Xie J, Zeng Y, Wang J, Zhang L. Optic nerve head perfusion changes preceding peripapillary retinal nerve fibre layer thinning in preclinical diabetic retinopathy. *Clin Exp Ophthalmol* 2019;47(2):219-225.

15 Shin YI, Nam KY, Lee SE, Lee MW, Lim HB, Jo YJ, Kim JY. Peripapillary microvasculature in patients with diabetes mellitus: an optical coherence tomography angiography study. *Sci Rep* 2019;9(1):15814.

16 Wu Y, Yang Q, Ding L, Tu Y, Deng X, Yang Y, Shen M, Lu Q, Lu F, Chen Q. Peripapillary structural and microvascular alterations in early dysthyroid optic neuropathy. *Eye Vis (Lond)* 2022;9(1):30.

17 Yılmaz Tuğan B, Sönmez HE. Optical coherence tomography angiography of subclinical ocular features in pediatric Behçet disease. *J AAPOS* 2022;26(1):24.e1-24.24.e6.

18 Huynh SC, Wang XY, Burlutsky G, Mitchell P. Symmetry of optical coherence tomography retinal measurements in young children. *Am J Ophthalmol* 2007;143(3):518-520.

19 Murdoch IE, Morris SS, Cousens SN. People and eyes: statistical approaches in ophthalmology. *Br J Ophthalmol* 1998;82(8):971-973.

20 Fishman RS. Optic disc asymmetry. A sign of ocular hypertension. *Arch Ophthalmol* 1970;84(5):590-594.

21 Mwanza JC, Durbin MK, Budenz DL, Cirrus OCT Normative Database Study Group. Interocular symmetry in peripapillary retinal nerve fiber layer thickness measured with the Cirrus HD-OCT in healthy eyes. *Am J Ophthalmol* 2011;151(3):514-521.e1.

22 Sugimoto M, Ito K, Goto R, Uji Y. Symmetry analysis for detecting early glaucomatous changes in ocular hypertension using optical coherence tomography. *Jpn J Ophthalmol* 2004;48(3):281-286.

23 Fang D, Tang F, Huang H, Cheung C, Chen H. Repeatability, interocular correlation and agreement of quantitative swept-source optical coherence tomography angiography macular metrics in healthy subjects. *Br J Ophthalmol* 2019;103(3):415-420.

24 Bland JM. How can I decide the sample size for a repeatability study? http://www-users.york.ac.uk/~mb55/meas/sizerep.htm. 2010.

25 Liao JJ. Sample size calculation for an agreement study. *Pharm Stat* 2010;9(2):125-132.

26 Stanga PE, Tsamis E, Papayannis A, Stringa F, Cole T, Jalil A. Swept-source optical coherence tomography Angio™ (Topcon Corp, Japan): technology review. *Dev Ophthalmol* 2016;56:13-17.

27 Koutsiaris AG, Batis V, Liakopoulou G, Tachmitzi SV, Detorakis ET, Tsironi EE. Optical Coherence Tomography Angiography (OCTA) of the eye: a review on basic principles, advantages, disadvantages and device specifications. *Clin Hemorheol Microcirc* 2023;83(3): 247-271.

28 Wang YM, Shen R, Lin TPH, Chan PP, Wong MOM, Chan NCY, Tang F, Lam AKN, Leung DYL, Tham CCY, Cheung CY. Optical coherence tomography angiography metrics predict normal tension glaucoma progression. *Acta Ophthalmol* 2022;100(7):e1455-e1462.

29 Lin TPH, Wang YM, Ho K, Wong CYK, Chan PP, Wong MOM, Chan NCY, Tang FY, Lam A, Leung DYL, Wong TY, Cheng CY, Cheung CY, Tham CC. Global assessment of arteriolar, venular and capillary changes in normal tension glaucoma. *Sci Rep* 2020;10(1):19222.

30 Shen R, Wang YM, Cheung CY, Chan PP, Tham CC. Comparison of optical coherence tomography angiography metrics in primary angle-closure glaucoma and normal-tension glaucoma. *Sci Rep* 2021;11(1):23136.

31 Karakosta A, Vassilaki M, Plainis S, Elfadl NH, Tsilimbaris M, Moschandreas J. Choice of analytic approach for eye-specific outcomes: one eye or two? *Am J Ophthalmol* 2012;153(3):571-579.e1.

32 Armstrong RA. Statistical guidelines for the analysis of data obtained from one or both eyes. *Ophthalmic Physiol Opt* 2013;33(1):7-14.

33 Ying GS, Maguire MG, Glynn R, Rosner B. Tutorial on biostatistics: statistical analysis for correlated binary eye data. *Ophthalmic Epidemiol* 2018;25(1):1-12.

34 Fernández-Vigo JI, Kudsieh B, Shi H, De-Pablo-Gómez-de-Liaño L, Serrano-Garcia I, Ruiz-Moreno JM, Martínez-de-la-Casa JM, García-Feijóo J, Fernández-Vigo JÁ. Normative database of peripapillary vessel density measured by optical coherence tomography angiography and correlation study. *Curr Eye Res* 2020;45(11):1430-1437.

35 Martus P. Statistical methods for the evaluation of diagnostic measurements concerning paired organs. *Stat Med* 2000;19(4):525-540.

36 WuDunn D, Takusagawa HL, Sit AJ, Rosdahl JA, Radhakrishnan S, Hoguet A, Han Y, Chen TC. OCT angiography for the diagnosis of glaucoma: a report by the American academy of ophthalmology. *Ophthalmology* 2021;128(8):1222-1235.

37 Hou H, Moghimi S, Zangwill LM, Shoji T, Ghahari E, Manalastas PIC, Penteado RC, Weinreb RN. Inter-eye asymmetry of optical coherence tomography angiography vessel density in bilateral glaucoma, glaucoma suspect, and healthy eyes. *Am J Ophthalmol* 2018;190:69-77.

38 Xu H, Zong Y, Zhai R, Kong X, Jiang C, Sun X. Intereye and intraeye asymmetry analysis of retinal microvascular and neural structure parameters for diagnosis of primary open-angle glaucoma. *Eye (Lond)* 2019;33(10):1596-1605.

39 Munk MR, Giannakaki-Zimmermann H, Berger L, Huf W, Ebneter A, Wolf S, Zinkernagel MS. OCT-angiography: a qualitative and quantitative comparison of 4 OCT-A devices. *PLoS One* 2017;12(5):e0177059.

40 Alnawaiseh M, Brand C, Bormann E, Sauerland C, Eter N. Quantification of macular perfusion using optical coherence tomography angiography: repeatability and impact of an eye-tracking system. *BMC Ophthalmol* 2018;18(1):123.

41 Frizziero L, Parrozzani R, Londei D, Pilotto E, Midena E. Quantification of vascular and neuronal changes in the peripapillary retinal area secondary to diabetic retinopathy. *Br J Ophthalmol* 2021;105(11):1577-1583.

42 Liberek I, Chaberek S, Anielska E, Kowalska K, Ostrowski K. Symmetry of retinal vessel arborisation in normal and amblyopic eyes. *Ophthalmologica* 2010;224(2):96-102.

43 Akil H, Huang AS, Francis BA, Sadda SR, Chopra V. Retinal vessel density from optical coherence tomography angiography to differentiate early glaucoma, pre-perimetric glaucoma and normal eyes. *PLoS One* 2017;12(2):e0170476.

44 Lei J, Pei C, Wen C, Abdelfattah NS. Repeatability and reproducibility of quantification of superficial Peri-papillary capillaries by four different optical coherence tomography angiography devices. *Sci Rep* 2018;8(1):17866.

45 Fernández-Vigo JI, Kudsieh B, Macarro-Merino A, Arriola-Villalobos P, Martínez-de-la-Casa JM, García-Feijóo J, Fernández-Vigo JÁ. Reproducibility of macular and optic nerve head vessel density measurements by swept-source optical coherence tomography angiography. *Eur J Ophthalmol* 2020;30(4):756-763.